



# Forazoline A: Marine-Derived Polyketide with Antifungal In Vivo Efficacy\*\*

Thomas P. Wyche, Jeff S. Piotrowski, Yanpeng Hou, Doug Braun, Raamesh Deshpande, Sean McIlwain, Irene M. Ong, Chad L. Myers, Ilia A. Guzei, William M. Westler, David R. Andes, and Tim S. Bugni\*

**Abstract:** Forazoline A, a novel antifungal polyketide with in vivo efficacy against *Candida albicans*, was discovered using LCMS-based metabolomics to investigate marine-invertebrate-associated bacteria. Forazoline A had a highly unusual and unprecedented skeleton. Acquisition of  $^{13}\text{C}$ – $^{13}\text{C}$  gCOSY and  $^{13}\text{C}$ – $^{15}\text{N}$  HMQC NMR data provided the direct carbon–carbon and carbon–nitrogen connectivity, respectively. This approach represents the first example of determining direct  $^{13}\text{C}$ – $^{15}\text{N}$  connectivity for a natural product. Using yeast chemical genomics, we propose that forazoline A operated through a new mechanism of action with a phenotypic outcome of disrupting membrane integrity.

Fungal infections result in over 1.5 million deaths annually worldwide and cost \$12 billion to treat.<sup>[1]</sup> *Candida* spp. are the most common fungal infections, especially in intensive care units, in solid-organ transplant patients, and in blood- and marrow-transplant patients.<sup>[2]</sup> Of the more than one hundred known *Candida* spp., *Candida albicans* is the most common cause of fungal-born human disease.<sup>[2]</sup> *C. albicans* causes various infections, including candidiasis, which affects about 400 000 people per year, with an astonishingly high mortality rate between 46 and 75 %.<sup>[2]</sup>

While amphotericin B has remained the standard for treatment of severe systemic fungal infections, it suffers from low solubility and is associated with dose-limiting toxicity.<sup>[3]</sup>

The high mortality rate<sup>[2]</sup> combined with the continued rise in fungal resistance to current therapeutics<sup>[4]</sup> demonstrates the ever-present need for new therapeutics.

As part of a drug discovery program to discover novel antifungal therapeutics, we analyzed a collection of marine-invertebrate-associated bacteria using LCMS-based metabolomics in conjunction with disc diffusion assays. Metabolomics methodology has shown great promise for streamlining the discovery of novel natural products<sup>[5]</sup> and overcoming historic barriers such as the high rate of rediscovery of known compounds.<sup>[6]</sup>

Using metabolomics-based strategies which we previously published,<sup>[5]</sup> we analyzed LCMS profiles of 34 marine-derived bacterial extracts by principal component analysis (PCA) and identified the strain WMMB-499, an *Actinomyces* sp. cultivated from the ascidian *Ecteinascidia turbinata* (Herdman, 1880), as a metabolic outlier. After fermentation and subsequent purification, WMMB-499 was found to produce three distinct classes of novel compounds. The first class, halogenated electrophilic polyketides halomaduronones A–D which activate the Nrf2-ARE pathway, was recently described.<sup>[7]</sup> Forazoline A (**1**) and B (**2**), described herein, represented the second novel class. The third class was represented by a potent antibiotic, which is still under study. Forazoline A (**1**) was the lead antifungal agent with a highly unusual and unprecedented structure. Forazoline A (**1**)

[\*] T. P. Wyche, Dr. Y. Hou, D. Braun, Prof. Dr. T. S. Bugni  
Pharmaceutical Sciences Division  
University of Wisconsin-Madison, Madison, WI 53705 (USA)  
E-mail: tbugni@pharmacy.wisc.edu

Dr. J. S. Piotrowski, S. McIlwain, I. M. Ong  
Great Lakes Bioenergy Research Center  
University of Wisconsin-Madison, Madison, WI 53726 (USA)  
R. Deshpande, C. L. Myers  
Department of Computer Science and Engineering, University of  
Minnesota-Twin Cities, Minneapolis, MN 55455 (USA)

Dr. I. A. Guzei  
Department of Chemistry, University of Wisconsin-Madison  
Madison, WI 53706 (USA)

Dr. W. M. Westler  
Department of Biochemistry, University of Wisconsin-Madison  
Madison, WI 53706 (USA)

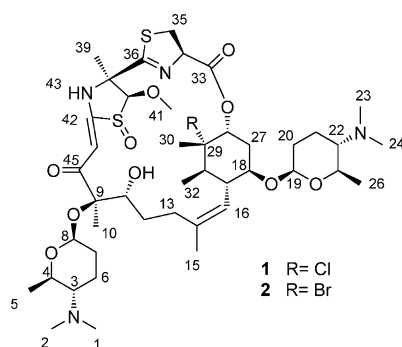
Prof. Dr. D. R. Andes  
School of Medicine, University of Wisconsin-Madison  
Madison, WI 53705 (USA)

[\*\*] We acknowledge financial support from the University of Wisconsin-Madison School of Pharmacy. This work was also funded by the NIH, NIGMS Grant R01 GM092009, and in part by R01 GM104192.

J.P., I.O., and S.M. are funded by the DOE Great Lakes Bioenergy Research Center (DOE BER Office of Science DE-FC02-07ER64494). C.M. and R.D. are supported by grants from the National Institutes of Health (1R01HG005084-01A1, 1R01M104975-01, R01HG005853), a grant from the National Science Foundation (DBI 0953881), and by the CIFAR Genetic Networks Program. We would like to thank the Analytical Instrumentation Center at the University of Wisconsin-Madison for the facilities to acquire spectroscopic data. This study made use of the National Magnetic Resonance Facility at Madison, which is supported by NIH grants P41RR02301 (BRT/NCRR) and P41M66326 (NIGMS). Additional equipment was purchased with funds from the University of Wisconsin, the NIH (RR02781, RR08438), the NSF (DMB-8415048, OIA-9977486, BIR-9214394), and the USDA. We would like to thank D. Demaria for assistance with collection and Dr. R. McClain for assistance with ICP-AES. The yeast deletion collection was kindly provided by Charlie Boone. CD data were obtained at the University of Wisconsin-Madison Biophysics Instrumentation Facility, which was established with support from the University of Wisconsin and grants BIR-9512577 (NSF) and S10RR13790 (NIH).



Supporting information for this article is available on the WWW under <http://dx.doi.org/10.1002/anie.201405990>.



demonstrated *in vivo* efficacy against the fungal pathogen *Candida albicans* and works by a putative novel mechanism. Forazoline B (**2**), a brominated analogue, was also produced to aid in structure elucidation.

Analysis of forazoline A (**1**) by HRMS supported the molecular formula of  $C_{43}H_{69}ClN_4O_{10}S_2$ . The MS isotopic distribution suggested the presence of one chlorine atom and two sulfur atoms. HRMS of **1** in  $CD_3OD$  and  $D_2O$  revealed the presence of two exchangeable protons. Acquisition of a  $^1H$ - $^{15}N$  HSQC allowed us to conclude that one of the exchangeable protons was on an enamine ( $\delta_H = 14.58$  ppm,  $\delta_N = 70.3$  ppm). To determine the location of the other exchangeable proton, **1** was acetylated.<sup>[8]</sup> Two major products, mono- and bis(acetyl) analogues were formed, and acquisition of one-dimensional (1D) and two-dimensional (2D) NMR spectra determined that the other exchangeable proton was an OH at C11.

Extensive 1D and 2D NMR data<sup>[8]</sup> (see Table S14 in the Supporting Information) were analyzed to establish the majority of the planar structure. However, the structure elucidation presented several challenges. Therefore, we unambiguously determined the carbon backbone by fermentation with uniformly labeled  $^{13}C$  glucose and acquisition of a  $^{13}C$ - $^{13}C$  gCOSY spectra, an approach we previously demonstrated as useful for determining carbon-carbon connectivity.<sup>[9]</sup> Fermentation of WMMB-499 with  $^{13}C$ -labeled glucose yielded **1** with approximately 75 %  $^{13}C$  incorporation. The  $^{13}C$ - $^{13}C$  gCOSY spectra was acquired in 30 minutes on 7.0 mg of **1** and allowed complete assignment of the carbon backbone.

To help confirm the location of the chlorine atom, the amount of KBr in the fermentation medium ASW-A was increased from  $0.1\text{ g L}^{-1}$  to  $10\text{ g L}^{-1}$  to produce the brominated analogue **2**. HRMS of **2** supported the molecular formula  $C_{43}H_{69}BrN_4O_{10}S_2$ . A comparison of the  $^1H$  and  $^{13}C$  NMR shifts of **1** and **2** showed that for **2** the chemical shifts of H28, H31, C28, and C31 shifted downfield, and C29 shifted upfield.<sup>[8]</sup> No other significant changes in chemical shifts between **1** and **2** existed, and we concluded that the halogen atom was located at C29.

As a result of the unique nature of the thiazoline-type rings, we pursued direct determination of  $^{13}C$ - $^{15}N$  connectivity, which had not been achieved for a natural product. Fermentation of 250 mL of WMMB-499 with  $^{15}NH_4Cl$  and uniformly labeled  $^{13}C$ -glucose, provided  $^{13}C$ - and  $^{15}N$ -labeled **1**. A  $^{13}C$ - $^{15}N$  HMQC ( $J_{CN}$  15 Hz) spectra was then acquired to determine the  $^{13}C$ - $^{15}N$  connectivity. The spectrum revealed

that N43 ( $\delta = 140.2$  ppm) was attached to C42 ( $\delta = 166.5$  ppm) and C38 ( $\delta = 76.2$  ppm), and N37 ( $\delta = 302.6$  ppm) was attached to C36 ( $\delta = 170.3$  ppm) and C34 ( $\delta = 76.3$  ppm). The spectrum also confirmed the presence of two N-dimethyl groups. The downfield shift of N37 and the downfield shift of C36, combined with the  $^{13}C$ - $^{15}N$  correlations, confirmed the thiazoline structure.

While analysis of the  $^{13}C$ - $^{13}C$  COSY and  $^{13}C$ - $^{15}N$  HMQC data rapidly provided the majority of the planar structure, additional data were necessary to complete structure elucidation. The presence of the sulfoxide was indicated by an absorption in the IR spectrum at  $1060\text{ cm}^{-1}$ . Additionally, having accounted for all carbon substituents, logically, the remaining oxygen atom was likely attached to the sulfur atom. Apratoxin, isolated from the marine cyanobacterium *Lyngbya majuscula*,<sup>[10]</sup> had a thiazoline ring. And more recently, apratoxin sulfoxide, which contains a thiazoline moiety with a sulfoxide, was isolated.<sup>[11]</sup> The  $^{13}C$  NMR shift of the thiazoline methylene in apratoxin and apratoxin sulfoxide was  $\delta = 37.6$  and  $58.3$  ppm, respectively. The  $^{13}C$  NMR shift of the thiazoline methylene (C35) in **1** was  $\delta = 38.8$  ppm, similar to that of apratoxin and indicating that the sulfoxide was most likely not part of the thiazoline moiety in **1**. To support this hypothesis, low-energy conformers of the two possible regioisomers were determined with Spartan10,<sup>[12]</sup> and DFT NMR calculations (Gaussian09<sup>[13]</sup>) of the low energy conformers were analyzed with the DP4 probability method. The DP4 method uses a mathematical algorithm to compare calculated and experimental NMR shifts and determine which structure fits the experimental data better.<sup>[14]</sup> It should be noted that these modeling studies were done after much of the configuration had been established as outlined below. Each of the two possible sulfoxide diastereomers was also investigated using Spartan10 and Gaussian09.<sup>[8]</sup> After comparing the calculated  $^{13}C$  chemical shifts of the two structures and the corresponding set of diastereomers with the observed chemical shifts of **1**, the DP4 probability method predicted a 100.0 % probability that the sulfoxide was attached to C40 and C42. Notably, for the structure with the sulfoxide in the thiazoline moiety, DFT calculations resulted in a  $^{13}C$  chemical shift of  $\delta = 58.6$  ppm for C35, which is nearly identical to the methylene in apratoxin sulfoxide (Figure 1). Meanwhile, DFT calculations for **1** predicted a  $^{13}C$  chemical shift of  $\delta = 43.3$  ppm at C35. Thus, the location of the sulfoxide in **1** was supported by both chemical shifts of known compounds and DFT calculations.

The configuration of **1** was determined by a combination of NOE studies, coupling constant analysis, extensive molecular modeling, and DFT calculations. We began by determining the relative configuration of the two sugars by analyzing

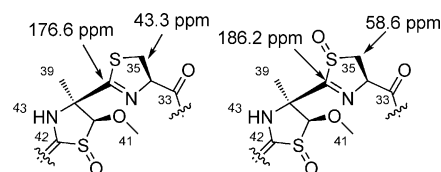
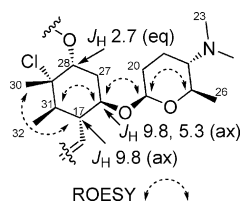


Figure 1. DFT-calculated  $^{13}C$  NMR shifts.



**Figure 2.** Key ROESY correlations and coupling constants.

NOE correlations and coupling constants as well as comparing  $^{13}\text{C}$  NMR shifts of sugars in known compounds. We then assigned the configuration of the chlorine-containing cyclohexane ring using a combination of NOE correlations and coupling constants (Figure 2). The configuration of the heterocyclic system (C34 to C42) was then investigated by molecular modeling and double-pulsed field-gradient-selective excitation (DPFGSE) NOE studies. The DPFGSE NOE experiment is advantageous over traditional 1D NOE experiments in that it provides a cleaner spectrum, thus greatly improving distance estimates.<sup>[15]</sup> In parallel, the configuration between C9 and C11 was assigned based on extensive molecular modeling and careful NOE studies. In addition, the configuration of the sulfoxide was determined by molecular modeling and DFT calculations.<sup>[8]</sup> Thus, convergent studies with NOE data, molecular modeling, and DFT calculations, which is detailed in the Supporting Information, allowed the assignment of the relative configuration of **1**.

Forazoline A (**1**) and B (**2**) demonstrated in vitro activity against *C. albicans* K1 with a minimum inhibitory concentration of  $16\ \mu\text{g mL}^{-1}$ . In vivo studies were pursued because of the relatively high aqueous solubility (ca.  $5\ \text{mg mL}^{-1}$ ). The compound **1** demonstrated in vivo efficacy in neutropenic (immunocompromised) mice in a disseminated candidiasis model against *Candida albicans* K1.<sup>[16]</sup> Mice were treated with **1** at concentrations of 2.5, 0.78, and  $0.125\ \text{mg kg}^{-1}$ . After eight hours, the mice treated with the compound showed a decrease of greater than  $1\ \log_{10}\text{cfu/kidney}$  ( $1.5 \pm 0.12$ ) reduction in organism burden compared to that of the control mice. No toxic effects from the compound were apparent.

Chemical genomic profiling with the yeast, *Saccharomyces cerevisiae*, was used to investigate the mechanism of action of **1**. This method has been used to explore the mechanism of action for bioactive compounds, including natural products.<sup>[17]</sup> The compound **1** was screened against over four thousand deletion mutant yeast strains, genomic DNA was extracted, and mutant-specific DNA barcodes were amplified and sequenced by Illumina sequencing. Mutants sensitive to and resistant to **1** were determined by quantification of DNA barcodes, thus providing a chemical genomic profile which was used to evaluate the mechanism of action.

The compound **1** gave a distinct chemical genomic profile at  $250\ \mu\text{g mL}^{-1}$ . The top sensitive mutant strains ( $P < 0.0001$ ) were significantly enriched for genes involved in phospholipid translocation (GO: 0045332,  $P = 0.0009$ ). This enrichment was driven by sensitive mutants with deletions of the genes *LEM3* and *FPK1*. Lem3p forms a complex with Dnf1p/Dnf2p which is responsible for maintaining phospholipid asymmetry in membranes while Fpk1p is a Ser/Thr protein kinase which regulates Lem3p-Dnf1p/Dnf2p (Dnf1p is a phospholipid translocase).<sup>[18]</sup> These data suggest that **1** either directly affects phospholipids or interacts with a protein target which complements the activity of the Lem3p complex. An impor-

tant aspect of these data was that *LEM3-Δ* was not among the most sensitive strains for caspofungin, fluconazole, or amphotericin, thus suggesting that **1** has a unique mechanism of action from known antifungal agents.

Among the top mutant strains resistant to **1** ( $P < 0.0001$ ), we saw significant enrichment for genes involved in negative regulation of chromatin silencing at rDNA (GO:0061188,  $P = 0.002$ ), driven by mutants of *SDS3* and *DEP1* which encode proteins involved with the regulation of phospholipid biosynthesis. Dep1 is a transcriptional modulator involved in the regulation of phospholipid biosynthesis.<sup>[19]</sup>

We then compared the chemical genomic profile of **1** to existing chemical genomic datasets<sup>[20]</sup> and our unpublished dataset, and found its profile significantly correlated with that of papuamide B and tyrocidine B ( $P < 0.0001$ ). Both of these compounds act by damaging cellular membranes and causing cell leakage.<sup>[21,22]</sup> Taken together, these data suggested that **1** affected membrane integrity. In contrast, the top 50 sensitive mutant strains for papuamide B, for example, did not contain deletions of *LEM3* or *FPK1*,<sup>[20]</sup> thus indicating that **1** likely has a different mechanism of action than compared to that of papuamide B, which targets phosphatidylserine.

To investigate the membrane integrity of yeast cells treated with **1**, we evaluated membrane permeability. The compound **1** caused a dose-dependent permeabilization of fungal membranes after four hours of treatment (Figure 3),

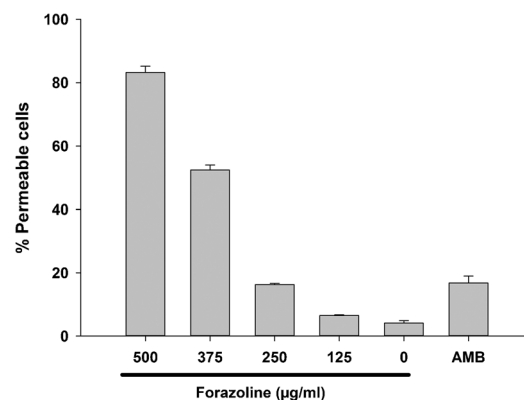


**Figure 3.** Forazoline A (**1**) compromises membrane integrity in a dose-dependent manner. Forazoline A (**1**) caused cell permeability after 4 h of treatment, and membrane damage increased with the concentration. Amphotericin B (AMB) was included as a positive control which causes cell leakage by binding ergosterol in fungal membranes. (Mean  $\pm$  standard error.)

but was less potent than amphotericin. Since chemical genomics suggested that **1** had a different mechanism compared to that of amphotericin, we further evaluated the hypothesis through synergy studies. The compound **1** showed synergy when tested with amphotericin, thus indicating a parallel and/or complementary mechanism of action. The data indicated that membrane integrity was affected by **1**, but additional studies will be necessary to fully unravel the details surrounding mechanism of action.

Given the rising resistance to antifungal agents, there is a pressing need for new antifungal agents with novel mechanisms of action. The compound **1**, a complex, novel natural product from a marine-derived *Actinomadura* sp., represents a new class of antifungal natural products and demonstrated in vivo efficacy—comparable to that of amphotericin B—in a mouse model of *C. albicans* and no toxicity. Additionally, combination treatment of **1** and amphotericin B demonstrated a synergistic effect in vitro. A chemical genomic approach suggested that **1** affects cell membranes, possibly through dysregulation of phospholipid homeostasis. While additional studies are necessary to better characterize the mechanism of action, **1** represents a promising antifungal agent with a new mechanism of action compared to that of the current clinically approved agents.

Received: June 6, 2014

Published online: September 4, 2014

**Keywords:** antifungal agents · genomics · natural products · NMR spectroscopy · structure elucidation

- [1] R. Zaragoza, J. Peman, *Adv. Sepsis* **2008**, 6, 90–98.
- [2] S. Giri, A. J. Kindo, *Indian J. Med. Microbiol.* **2012**, 30, 270–278.
- [3] a) J. P. Barrett, K. A. Vardulaki, C. Conlon, J. Cooke, P. Daza-Ramirez, E. G. V. Evanas, P. M. Hawkey, R. Herbrecht, D. I. Marks, J. M. Moraleda, G. R. Park, S. J. Senn, C. Viscoli, *Clin. Ther.* **2003**, 25, 1295–1320; b) R. Laniado-Laborin, M. N. Cabrales-Vargas, *Rev. Iberoam Micol.* **2009**, 26, 223–227.
- [4] Z. A. Kanafani, J. R. Perfect, *Clin. Infect. Dis.* **2008**, 46, 120–128.
- [5] a) D. Krug, G. Zurek, O. Revermann, M. Vos, G. J. Velicer, R. Müller, *Appl. Environ. Microbiol.* **2008**, 74, 3058–3068; b) D. Krug, G. Zurek, B. Schneider, R. Garcia, R. Müller, *Anal. Chim. Acta* **2008**, 624, 97–106; c) Y. Hou, D. R. Braun, C. R. Michel, J. L. Klassen, N. Adnani, T. P. Wyche, T. S. Bugni, *Anal. Chem.* **2012**, 84, 4277–4283.
- [6] “The Need for New Antibiotics”: H. Zäehner, H. P. Fiedler in *Fifty Years of Antimicrobials* (Eds.: P. A. Hunter, G. K. Darby, N. J. Russel), Cambridge University Press, Cambridge, England, **1995**, pp. 67–84.
- [7] T. P. Wyche, M. Standiford, Y. Hou, D. Braun, D. A. Johnson, J. A. Johnson, T. S. Bugni, *Mar. Drugs* **2013**, 11, 5089–5099.
- [8] Complete characterization of forazoline A and B, including tabulated data and copies of the <sup>1</sup>H and <sup>13</sup>C NMR spectra, is provided in the Supporting Information.
- [9] G. A. Ellis, T. P. Wyche, C. G. Fry, D. R. Braun, T. S. Bugni, *Mar. Drugs* **2014**, 12, 1013–1022.
- [10] H. Luesch, W. Y. Yoshida, R. E. Moore, V. J. Paul, T. H. Corbett, *J. Am. Chem. Soc.* **2001**, 123, 5418–5423.
- [11] C. C. Thornburg, E. S. Cowley, J. Sikorska, L. A. Shaala, J. E. Ishmael, D. T. A. Youssef, K. L. McPhail, *J. Nat. Prod.* **2013**, 76, 1781–1788.
- [12] Spartan 10, v. 1.0.2. Wavefunction Inc. **2011**.
- [13] Gaussian09, Revision A.1, M. J. Frisch, G. W. Trucks, H. B. Schlegel, G. E. Scuseria, M. A. Robb, J. R. Cheeseman, G. Scalmani, V. Barone, B. Mennucci, G. A. Petersson *et al.*, Gaussian, Inc., Wallingford CT, **2009**.
- [14] S. G. Smith, J. M. Goodman, *J. Am. Chem. Soc.* **2010**, 132, 12946–12959.
- [15] K. Stott, J. Keeler, Q. N. Van, A. J. Shaka, *J. Magn. Reson.* **1997**, 125, 302–304.
- [16] Low yields for forazoline B (**2**) have prevented initial in vivo studies with the compound. In vivo studies of **2** will be reported in due course.
- [17] a) C. H. Ho, J. Piotrowski, S. J. Dixon, A. Baryshnikova, M. Costanzo, C. Boone, *Curr. Opin. Chem. Biol.* **2011**, 15, 66–78; b) A. B. Parsons, R. L. Brost, H. Ding, Z. Li, C. Zhang, B. Sheikh, G. W. Brown, P. M. Kane, T. R. Hughes, C. Boone, *Nat. Biotechnol.* **2004**, 22, 62–69; c) M. Costanzo, A. Baryshnikova, J. Bellay, Y. Kim, E. D. Spear, C. S. Sevier, H. Ding, J. L. Koh, K. Toufighi, S. Mostafavi *et al.*, *Science* **2010**, 327, 425–431; d) S.-Y. Fung, V. Sofiyev, J. Schneiderman, A. F. Hirschfeld, R. E. Victor, K. Woods, J. S. Piotrowski, R. Deshpande, S. C. Li, N. J. de Voogd, C. L. Myers, C. Boone, R. J. Andersen, S. E. Turvey, *ACS Chem. Biol.* **2014**, 9, 247–257.
- [18] K. Nakano, T. Yamamoto, T. Kishimoto, T. Noji, K. Tanaka, *Mol. Cell. Biol.* **2008**, 19, 1783–1797.
- [19] E. Lamping, J. Lückl, F. Paltauf, S. A. Henry, S. D. Kohlwein, *Genetics* **1994**, 137, 55–65.
- [20] A. B. Parsons, A. Lopez, I. E. Givoni, D. E. Williams, C. A. Gray, J. Porter, G. Chua, R. Sopko, R. L. Brost, C. H. Ho *et al.*, *Cell* **2006**, 126, 611–625.
- [21] P. W. Ford, K. R. Gustafson, T. C. McKee, N. Shigematsu, L. K. Maurizi, L. K. Pannell, D. E. Williams, E. D. de Silva, P. Lassota, T. M. Allen, R. Van Soest, R. J. Anderson, M. R. Boyd, *J. Am. Chem. Soc.* **1999**, 121, 5899–5909.
- [22] J. M. Merrick, *J. Bacteriol.* **1965**, 90, 965–969.